

# Supplemental Material to: Band structure of a HgTe-based three-dimensional topological insulator

J. Gospodarič,<sup>1</sup> V. Dziom,<sup>1</sup> A. Shuvaev,<sup>1</sup> A. A. Dobretsova,<sup>2</sup>  
N. N. Mikhailov,<sup>2</sup> Z. D. Kvon,<sup>2</sup> E. G. Novik,<sup>3,4</sup> and A. Pimenov<sup>1</sup>

<sup>1</sup>*Institute of Solid State Physics, Vienna University of Technology, 1040 Vienna, Austria*

<sup>2</sup>*Rzhanov Institute of Semiconductor Physics and Novosibirsk State University, Novosibirsk 630090, Russia*

<sup>3</sup>*Dresden High Magnetic Field Laboratory (HLD-EMFL),*

*Helmholtz-Zentrum Dresden-Rossendorf, 01328 Dresden, Germany*

<sup>4</sup>*Institute of Theoretical Physics, Technische Universität Dresden, 01062 Dresden, Germany*

In this Supplemental Material, we provide an extensive report of the experimentally acquired intensity of the transmitted radiation at various experimental conditions like gate voltage or incident frequency. Correspondingly, electrodynamic parameters of all resonances detected in the spectra are presented. Lastly, the influence of the bulk inversion asymmetry on the band structure calculation is demonstrated.

## MAGNETO-OPTICAL TRANSMISSION

As discussed in the main text, the magnetoelectric spectra contain multiple cyclotron resonance peaks. Not all of these resonances could be interpreted within the quasi-classical approximation as they showed non-monotonic gate-voltage dependence. In such cases it is difficult to attribute these resonances to a well-defined quasi-particle response and the procedure to calculate the band structure does not work. Additional resonances are most probably the result of direct transitions between Landau levels and they cannot be described within the quasi-classical picture. However, for completeness, in this Supplementary Material, we present the full set of the transmission spectra and the results of the Drude analysis of all the fitted resonances, even the ones that were not included in the calculation of the band structure.

Figure. SI.1 shows the transmission spectrum of HgTe film on a (100) GaAs substrate in zero magnetic field. The spectrum consists of three parts corresponding to three separate experiments with different BWO-generators. This spectrum was fitted using the Drude

model for the film conductivity which included the effects from the substrate. Since all fittings were performed simultaneously, the same parameters were used to fit the magnetic field dependence of the transmission. The oscillations in Fig. SI.1 are due to Fabry-Pérot interference in the substrate. The magnetic field-dependent experiments were carried out at frequencies close to the maxima of the Fabry-Pérot resonances as here the effect of the substrate is minimized<sup>1</sup>.

In the following we present an expanded set of field-dependent transmission curves which were measured at frequencies 142, 347 and 687 GHz and at different gate voltages. In these data sets, several resonances were observed and analyzed. The Drude model provided good fits of the experimental data. We recall that due to circular polarization of the incident radiation the resonances corresponding to hole-like carriers were observed at negative magnetic fields and the electron-like resonances in positive fields. Where possible, the labeling of the resonances was preserved for all frequencies and gate voltages by following gradual changes of their corresponding positions in field and intensities.

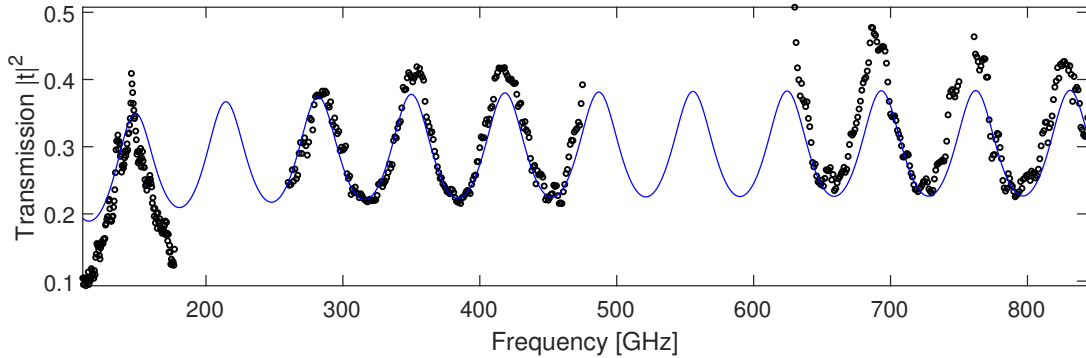


FIG. SI.1. Frequency dependent intensity of transmission of the HgTe film in zero magnetic field and at  $T = 1.8$  K. Open black circles - experiment, blue curve - fit using Fresnel optical equations and the Drude model. Substrate parameters are: thickness  $d = 0.608$  mm, refractive index  $n = 3.57$ .

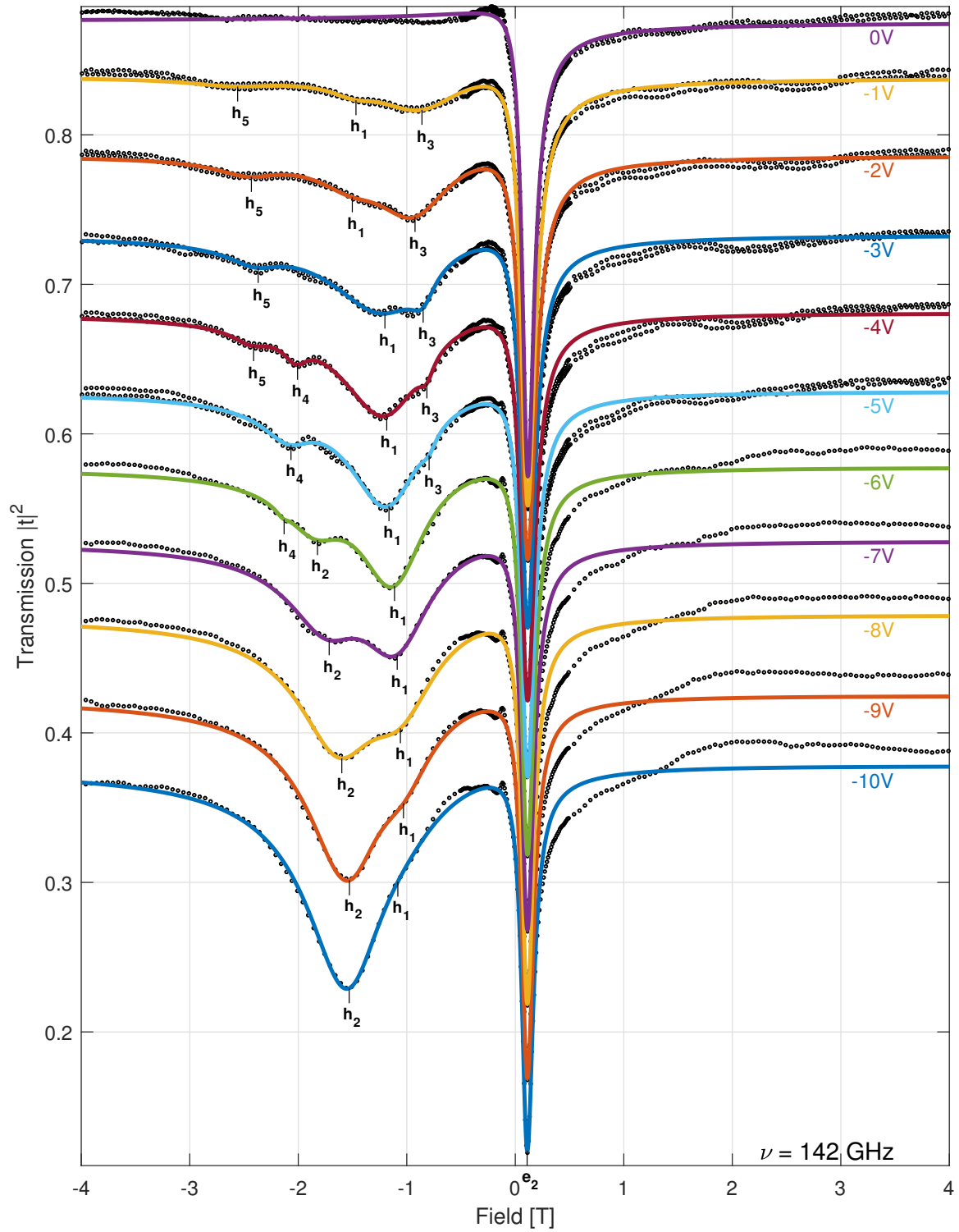


FIG. SI.2. The magneto-optical intensity of transmission spectra of circularly polarized radiation at 142 GHz and at  $T = 1.8$  K. The spectra obtained at different applied voltages are vertically shifted for clarity. Open black circles: experiment. Solid lines: fits of the transmission using the Drude model containing various charge carriers (see resonant peak labels). Holes appear at negative magnetic fields and electrons on the positive side.

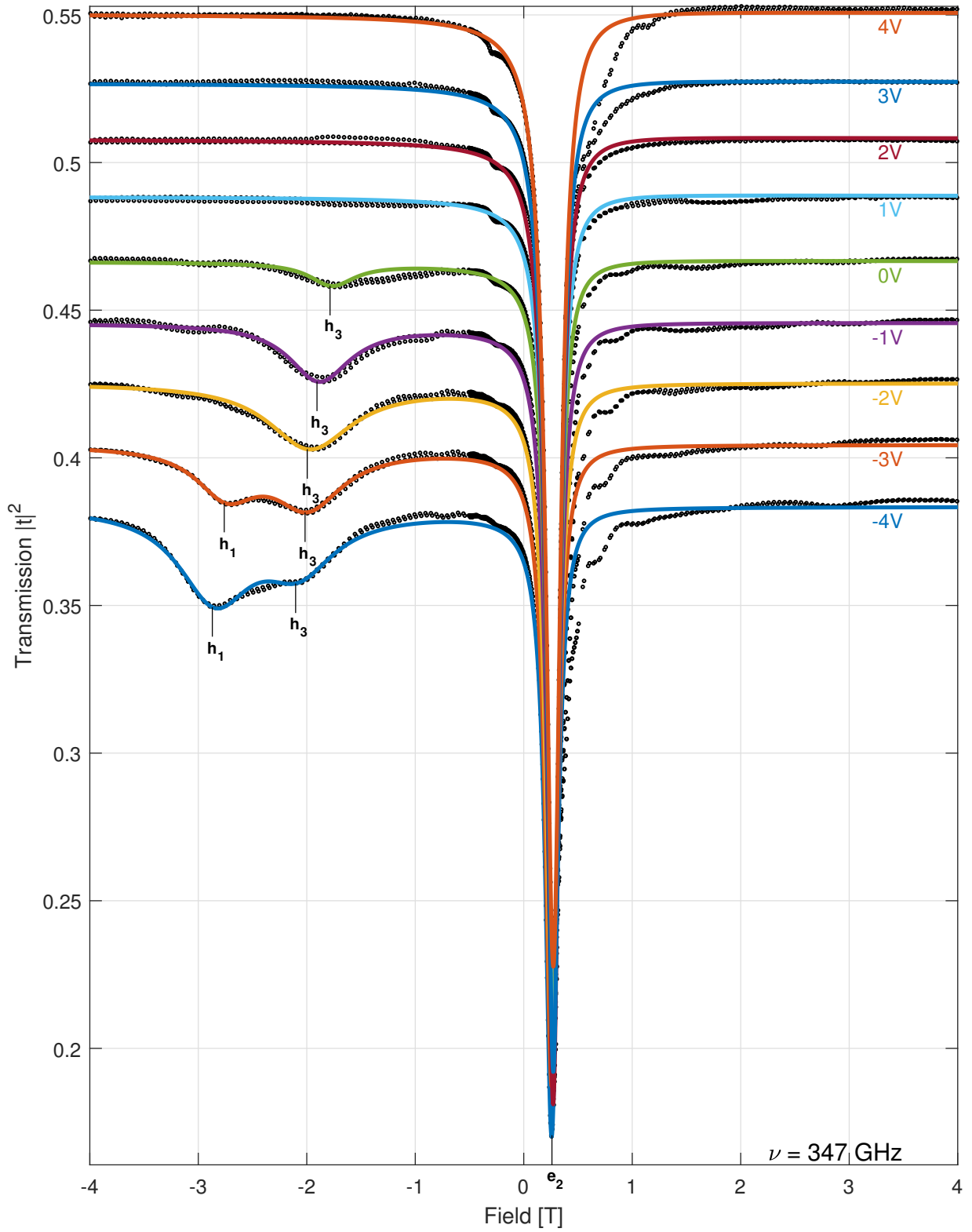


FIG. SI.3. The magneto-optical intensity of transmission spectra of circularly polarized radiation at 347 GHz and at  $T = 1.8$  K. The spectra obtained at different applied voltages are vertically shifted for clarity. Open black circles: experiment. Solid lines : fits of the transmission using the Drude model containing various charge carriers.

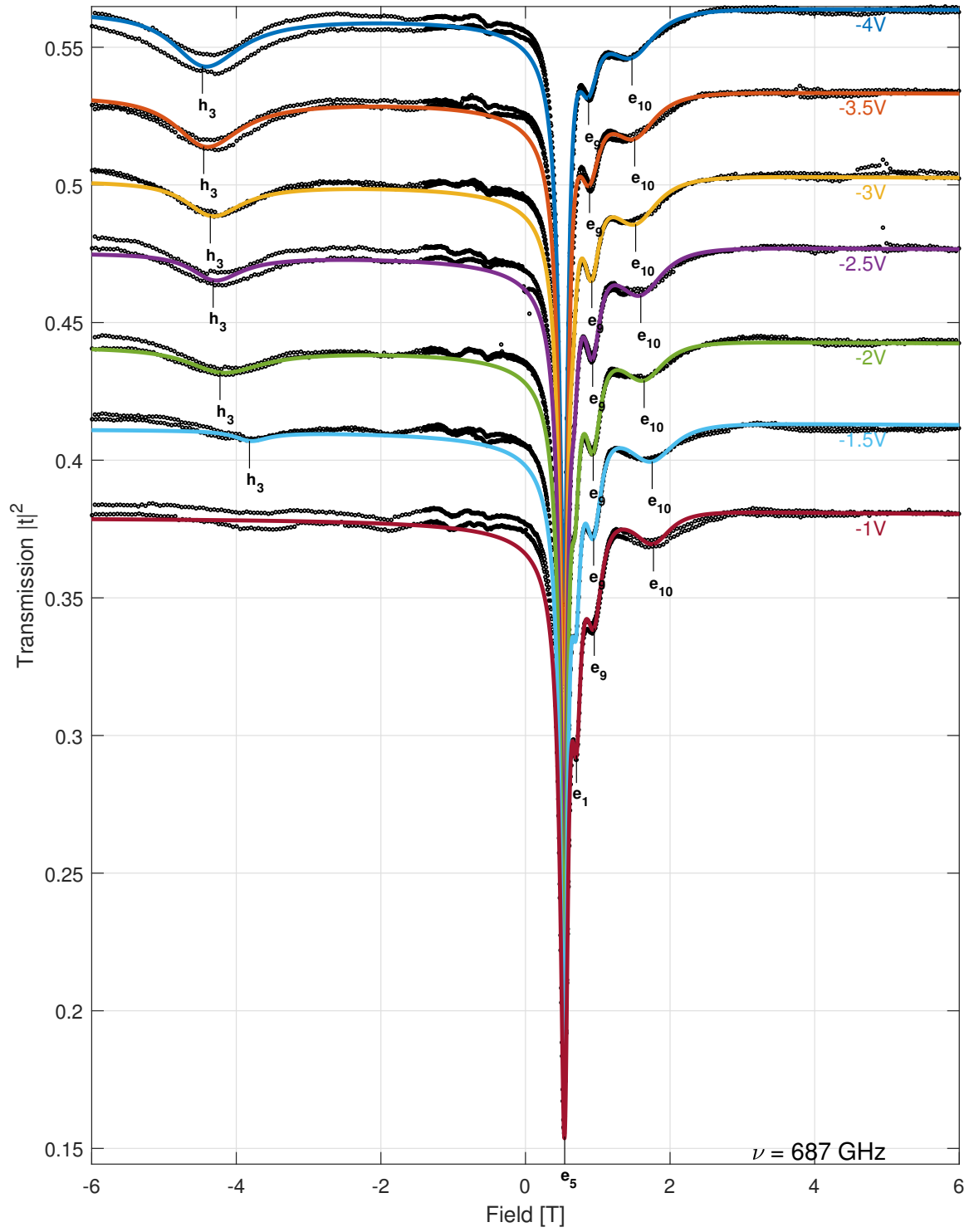


FIG. S1.4. The magneto-optical intensity of transmission spectra of circularly polarized radiation at 687 GHz and at  $T = 1.8$  K (full field range). The spectra obtained at different applied voltages are vertically shifted for clarity. Open black circles: experiment. Solid lines : fits of the transmission using the Drude model containing various charge carriers.

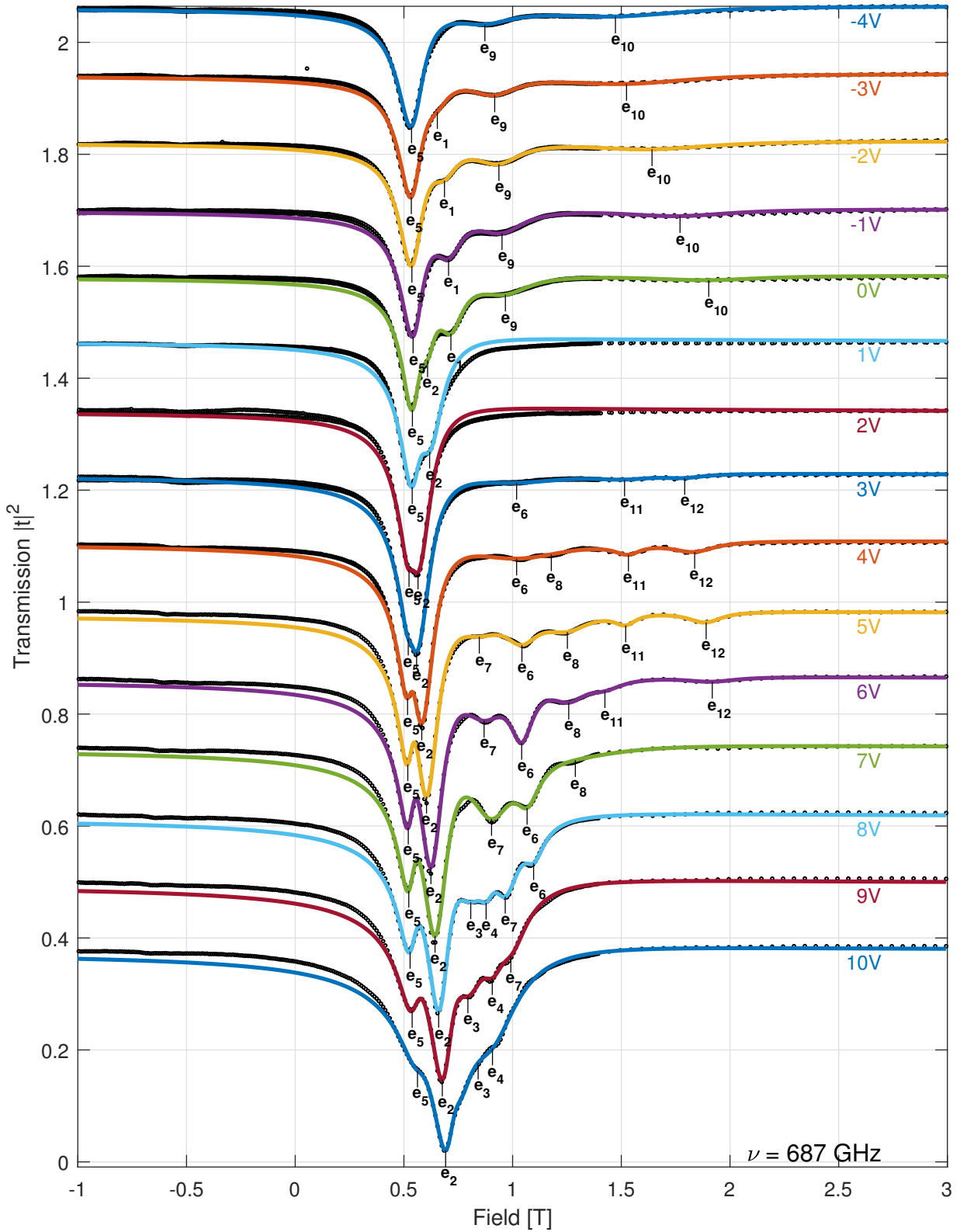


FIG. SI.5. The magneto-optical intensity of transmission spectra of circularly polarized radiation at 687 GHz and at  $T = 1.8$  K (expanded region of the electron-like carriers). The spectra obtained at different applied voltages are vertically shifted for clarity. Open black circles: experiment. Solid lines : fits of the transmission using the Drude model containing various charge carriers.

## ELECTRODYNAMIC PARAMETERS OF CYCLOTRON RESONANCES

Fitting the Drude model to the experimental data provided us with 2D electron density, effective cyclotron mass and scattering time of the charge carriers responsible for the resonant peaks. Resonances seen at multiple frequencies, similar gate regions and with overlapping effective masses and 2D densities were recognized as corresponding to the same carrier type and were therefore labeled as such (for example  $\mathbf{h}_3$  in Fig. SI.6).

However, as mentioned in the main text, not all detected resonant peaks were recognized as fingerprints of charged carriers. Their charge density had to either monotonically decrease (hole-like carriers) or increase (electron-like carriers) with increasing gate voltage. We observed such behavior only for carriers  $\mathbf{h}_2$ ,  $\mathbf{e}_1$ ,  $\mathbf{e}_2$ ,  $\mathbf{e}_3$ ,  $\mathbf{e}_4$ . In this section we also present the parameters of other resonances gathered from fitting the Drude model to the experimental transmission. The hole-like carriers are shown in Fig. SI.6 and electron-like carriers are separated into two parts: Fig. SI.7 (low masses,  $m_c/m_e < \sim 0.04$ ) and Fig. SI.8 (high masses).

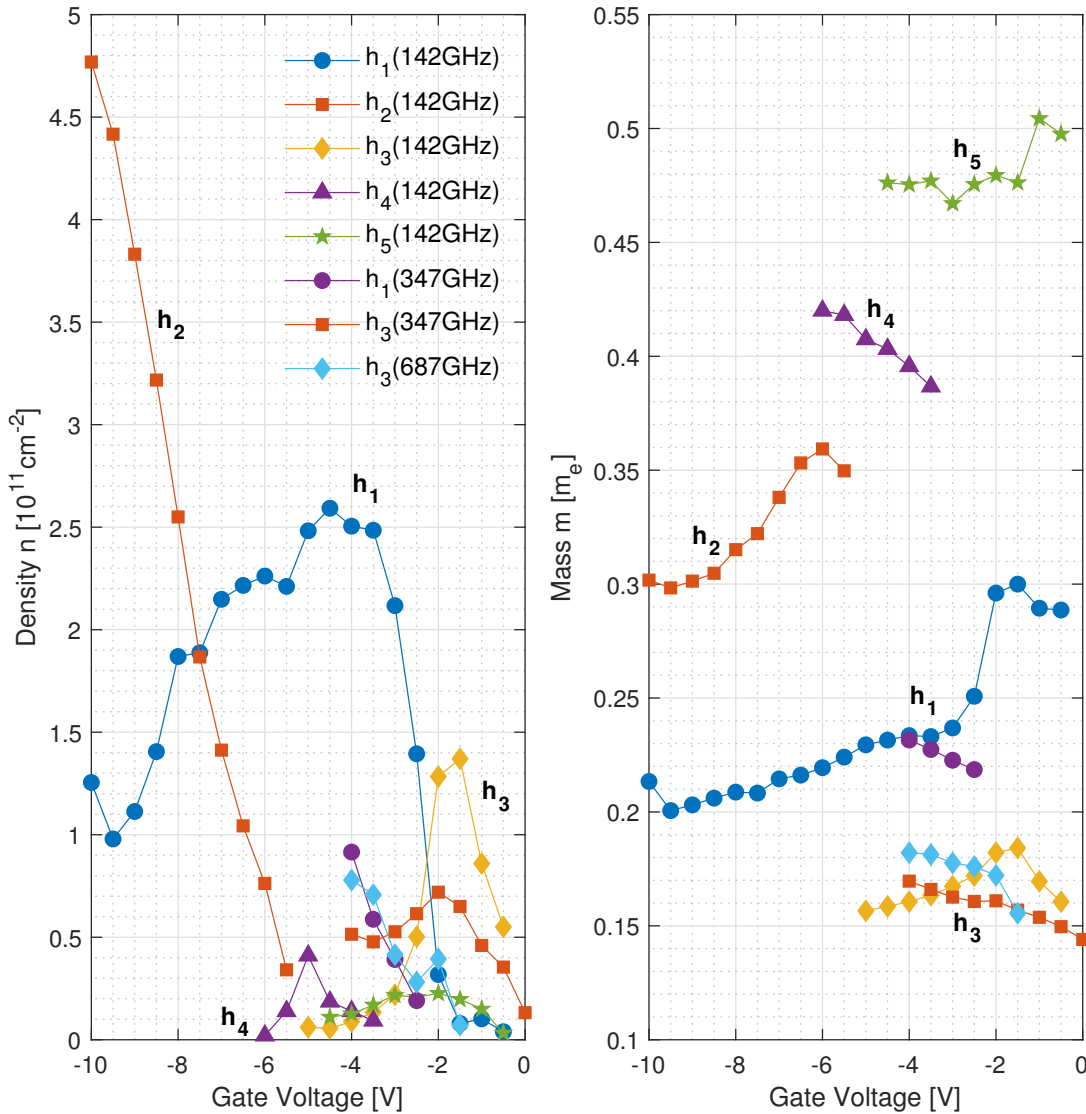


FIG. SI.6. Electrodynamic parameters of the hole-like cyclotron resonances in HgTe. Resonances were observed at frequencies as indicated in the legend.

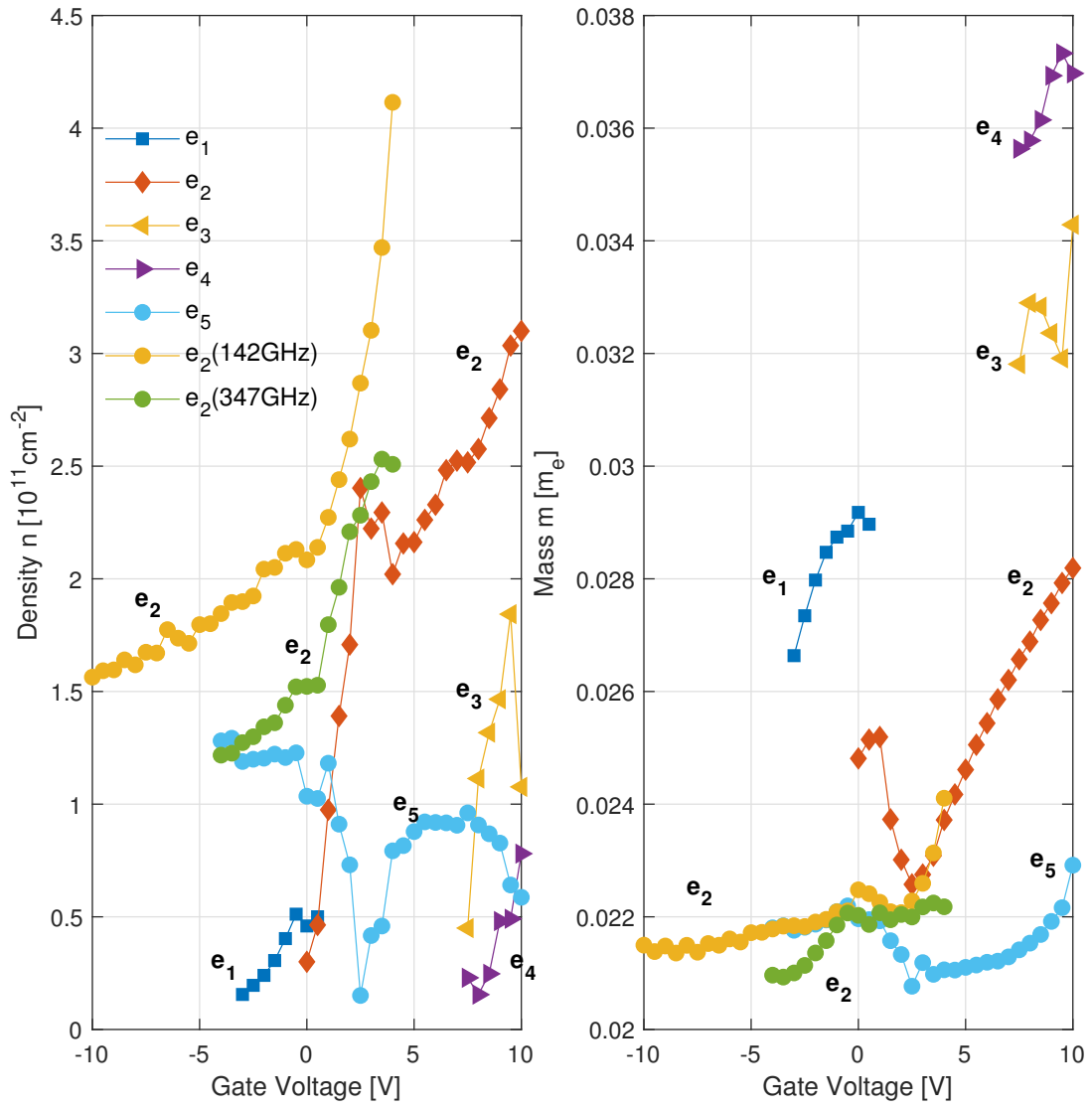


FIG. SI.7. Electrodynamic parameters of the electron-like cyclotron resonances in HgTe - Part 1. If not otherwise specified in the legend, the resonances were observed at 687 GHz.

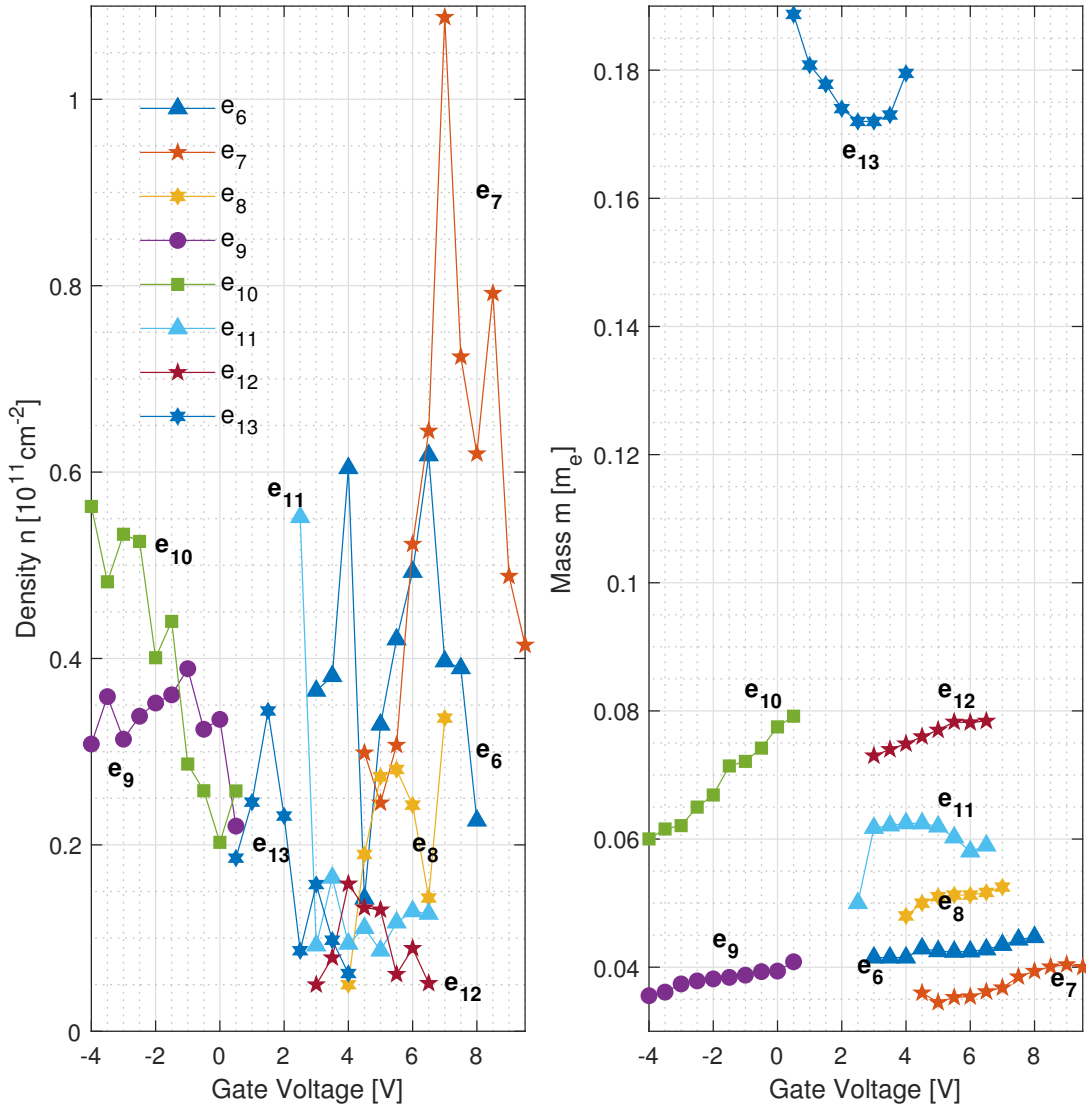


FIG. SI.8. Electrodynamic parameters of the electron-like cyclotron resonances in HgTe - Part 2. The resonances were observed at 687 GHz.

### BULK INVERSION ASYMMETRY CALCULATIONS

We have tested the influence of the bulk inversion asymmetry (BIA) terms on our model. The inclusion was tested when the system has charge neutrality ( $n_{tot} = 0$ ). It can be seen from Fig. SI.9 that the influence of the BIA

on the surface and electron-like states is small. On the other hand, BIA increases the energy of the holes around the valence band maxima. According to the experiment, see Fig. 5 of the main text, holes lie energetically at much lower energies. Since including BIA into consideration worsens agreement between theory and experiment, we did not include BIA in our calculations.

<sup>1</sup> V. Dziom, A. Shuvaev, A. Pimenov, G. V. Astakhov, C. Ames, K. Bendias, J. Böttcher, G. Tkachov, E. M. Hankiewicz, C. Brüne, H. Buhmann, and L. W. Molenkamp. Observation of the universal magnetoelectric effect in a 3D

topological insulator. *Nat. Commun.*, 8:15197, May 2017. URL <http://dx.doi.org/10.1038/ncomms15197>.

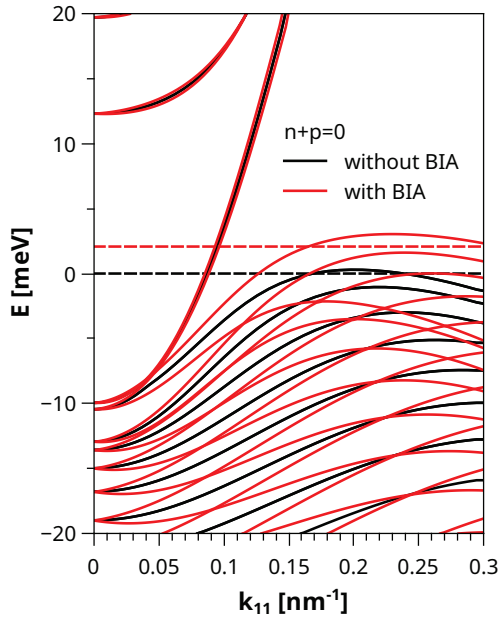


FIG. SI.9. Band structure calculation at  $n_{tot} = 0$ . The results of the model used in the main text (black data) are compared to the calculated dispersion of the model that includes the BIA term. Dashed lines show the position of the Fermi level for the charge neutrality point.